Structural and thermal properties of Xe on the Pb(111) surface studied by low-energy electron diffraction

2007 J. Phys.: Condens. Matter 19 056011

(http://iopscience.iop.org/0953-8984/19/5/056011)

INSTITUTE OF PHYSICS PUBLISHING JOURNAL OF PHYSICS: CONDENSED MATTER

J. Phys.: Condens. Matter **19** (2007) 056011 (12pp) doi:10.1088/0953-8984/19/5/056011

Structural and thermal properties of Xe on the Pb(111) surface studied by low-energy electron diffraction

N Ferralis[1], H I Li, K J Hanna, J Stevens, H Shin, F M Pan and R D Diehl[2]

Department of Physics, Penn State University, University Park, PA 16802, USA

E-mail: rdiehl@psu.edu

Received 13 November 2006, in final form 2 January 2007
Published 17 January 2007
Online at stacks.iop.org/JPhysCM/19/056011

Abstract

The growth, structures and thermodynamics of Xe adsorbed on Pb(111) were studied with low-energy electron diffraction (LEED). Measurements of equilibrium adsorption isobars indicate layer-by-layer growth for at least two layers in the temperature range 60–90 K, and an isosteric heat of adsorption of 191 ± 10 meV for the first Xe layer and 158 ± 20 meV for the second Xe layer. The monolayer has an incommensurate hexagonal structure with a lattice parameter similar to that found in bulk Xe, and its thermal expansion coefficient was measured to be $9 \pm 1 \times 10^{-4}$ K^{-1}. The average overlayer–substrate spacing was determined from a constant-momentum-transfer analysis of the LEED intensities to be 3.95 ± 0.10 Å. Vibrational information was obtained from measuring the decay of the diffraction intensities as a function of temperature. The perpendicular root mean square displacement of the Xe atoms at 50 K is 0.12 ± 0.01 Å, giving an effective Debye temperature for adsorbed Xe of 37 ± 2 K. The corresponding vibrational energy for the perpendicular mode of Xe is 3.2 ± 0.3 meV.

(Some figures in this article are in colour only in the electronic version)

1. Introduction

There is a growing interest in understanding the structures and dynamics of weakly interacting systems due to their importance in many areas of soft condensed matter and biological physics. Although they have been studied for many years, the interactions of gases physisorbed on surfaces are still not understood on a fundamental level. These systems have mostly eluded the dragnet of density functional theory (DFT) because, at this time, there is no widely accepted procedure for including the van der Waals interaction into such calculations. However, there

[1] Present address: Department of Chemical Engineering, 201 Gilman Hall, University of California, Berkeley, CA 94720-1462, USA.

[2] Author to whom any correspondence should be addressed.

is increasing activity toward this goal [1–3], and the test of such new theoretical developments depends on having experimentally measured quantities for comparison.

This paper describes a low-energy electron diffraction study of the adsorption of Xe on Pb(111). Xe adsorption on metal surfaces has been studied for some time [4], but most work on the surface geometries has been relatively recent [5]. Even without including the van der Waals interaction, a recent DFT study of Xe adsorption [6] was able to identify some trends in the bonding and adsorption geometries for Xe on many close-packed metal surfaces that are consistent with experimental studies. It had already been noted from experimental measurements that the Xe–metal distance decreases when the adsorption energy increases. A less obvious finding from the theoretical study is that the Xe–metal perpendicular spacing is largely insensitive to the adsorption site. This implies that the actual Xe to metal atom 'bond' distance depends strongly on the adsorption site, and that a hard-sphere model gives an inaccurate picture of Xe adsorption. The study presented here provides thermodynamic and structural information for Xe on Pb(111), which has not been addressed in previous studies, and compares these results to other similar systems.

2. Experiment

The experiments were carried out using an OCI^{TM} low-current LEED in an ultra-high vacuum (UHV) chamber that also has instrumentation for Auger electron spectroscopy (AES) and sample preparation. The sample manipulator incorporates an open-cycle He refrigerator for sample cooling.

The Pb(111) crystal was first polished using a diamond abrasive paste starting with 6 μm size grit and finishing with 0.25 μm size grit. The polishing was finished with 0.05 μm alumina. After the mechanical polishing, it was polished on a soft cloth with acetone for a few minutes, which gave it a shiny appearance. Two different chemical etching methods were used to prepare the Pb(111) surface before it was inserted into the UHV chamber. Both were effective, but the second produced a surface that required less preparation in UHV. In the first method, the Pb(111) sample was immersed for 1 min in a chemical etch that consisted a mixture of 25% acetic acid, 25% hydrogen peroxide and 50% water for a few minutes, giving the crystal surface a shiny appearance. Although the surface was visually good, it required more sputtering and annealing cycles to produce a good surface than the second method. In the second method, four different dipping solutions were used in succession. The first, the polishing solution, consisted of 2 ml of concentrated nitric acid, 100 ml of 5% acetic acid, 10 ml of saturated EDTA disodium salt solution and 5 ml of 30% hydrogen peroxide. The second solution was 10% saturated EDTA di-sodium salt solution. The third was 7.5% reagent grade ammonia, and the fourth was acetone. The crystal was dipped in each solution in turn for about 10 s each, the process was repeated four times, and finally it was dipped in just the polishing solution and then acetone. After this procedure, the surface had a matt appearance.

The crystal was then mounted onto a polished Cu plate, which was directly connected to the cryostat. The sample was heated using a resistive heater from LabWave Labs (maximum output 40 W) attached to the back of the Cu plate, and its temperature (T) was measured with a K-type thermocouple that was clamped to the surface of the sample. The thermocouple was calibrated at low T with a Si diode thermometer; the lowest temperature attained in these experiments was 11 K. The sample was prepared in UHV by repeated cycles of Ar^+-ion sputtering (1.0 keV, 1.0×10^{-4} mbar) for 15–30 min and annealing to about 230 °C for 5 min. An Auger electron spectroscopy (AES) spectrum of the surface before cleaning indicated that the main contaminant was carbon, but no impurities were detected after the cleaning procedure, as shown in figure 1.

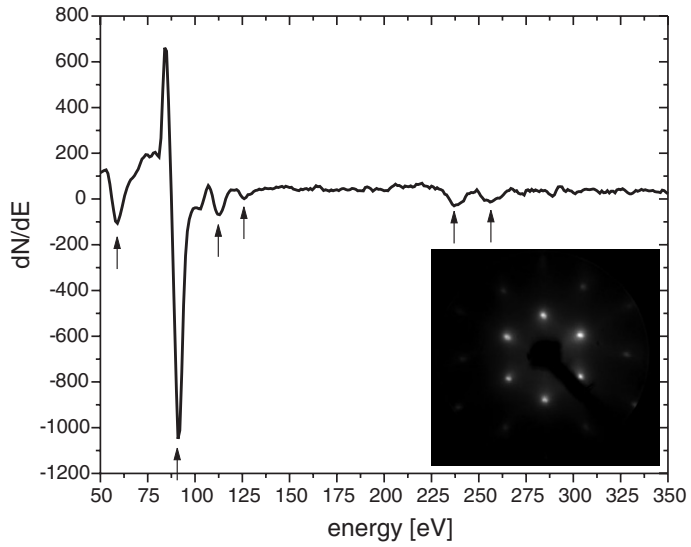

Figure 1. AES scans after the crystal preparation in UHV. Pb Auger peaks are marked with arrows. The LEED pattern ($E = 210$ eV) from the clean surface at $T = 30$ K is shown in the inset.

LEED data were acquired using a CCD video camera and data acquisition system that has been described previously [7]. For all of the measurements described here, whole frames (LEED patterns) were acquired and analysed later. The adsorption isobar measurements were performed by holding the Xe partial pressure in the UHV chamber constant while lowering or raising the sample temperature. In the isobar measurements, LEED patterns were acquired at incident beam energies of 79–98 eV. The intensities of the LEED spots were extracted from the frames using a circular integration window centred on the spot, and subtracting a background equal to the average intensity of the perimeter of the window.

The lattice parameters for the Xe overlayer were determined by measuring the distances between diffraction spots on the LEED pattern. Figure 2 shows the LEED pattern from a monolayer of Xe. The outer six spots are from the substrate, and the inner six azimuthally elongated spots are from the Xe monolayer. The positions of the diffraction spots from the Pb substrate and the known lattice constant of Pb were used to calibrate the lattice spacing measurements of the overlayer. The measurements were corrected for the flat geometry of the LEED screen. Lattice parameter measurements to determine the expansion coefficient were made for the constrained Xe monolayer, i.e. an overlayer in equilibrium with the three-dimensional (3D) Xe vapour.

The lattice vibration measurements were performed on 'unconstrained' layers, i.e. a partial monolayer with no Xe vapour. In order to produce unconstrained layers, the surface was cooled to 50 K, and Xe was leaked for a few seconds into the chamber at a pressure of 2.6×10^{-7} mbar until the incommensurate monolayer structure was observed in the LEED pattern. The Xe gas was then pumped away and the sample heated until the Xe was partially desorbed; this was determined by the reduction in intensity of the Xe spots. The film was then cooled again.

A constant momentum transfer analysis (CMTA), described in section 3.2, was carried out to determine the average Xe–Pb perpendicular spacing. This experiment involves measuring the intensity of the specular beam at various angles of incidence. For each angle, full LEED frames were acquired as a function of energy, and the intensities of the specular beam were later extracted as described above.

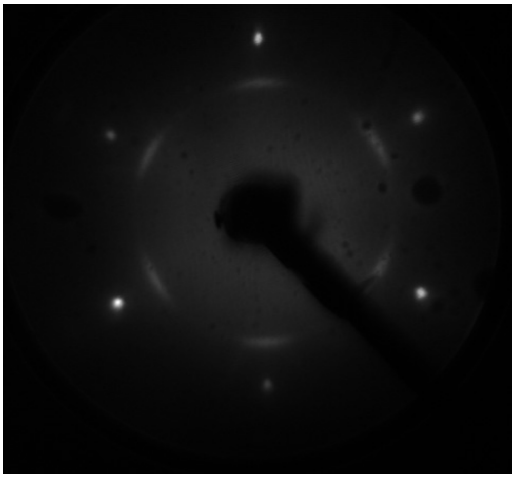

Figure 2. LEED pattern from a monolayer of Xe on Pb(111) at 75 eV and $T = 16$ K. The outer six spots are diffraction from the substrate lattice, the inner six (elongated) spots are from the Xe monolayer.

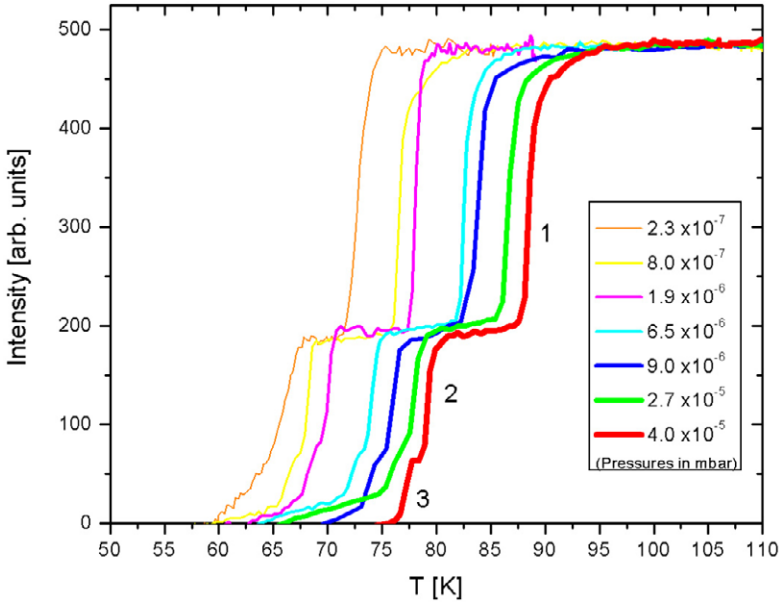

Figure 3. Xe adsorption isobars for Xe/Pb(111), showing the intensity of the substrate spots as a function of the sample temperature. The steps 1, 2 and 3 correspond to the first, second and third Xe layers, respectively. The intensities of three equivalent diffraction spots were averaged for each isobar. The curves are corrected for the Pb Debye–Waller factor. The Xe pressures are corrected using the normalization factor of the ion gauge for Xe (0.324).

3. Results

3.1. Thermodynamics of adsorption

Figure 3 shows isobaric measurements of the substrate diffraction intensity as a function of T in the Xe pressure range 2.3×10^{-7}–4.0×10^{-5} mbar. The isobars indicate a layer-by-layer growth

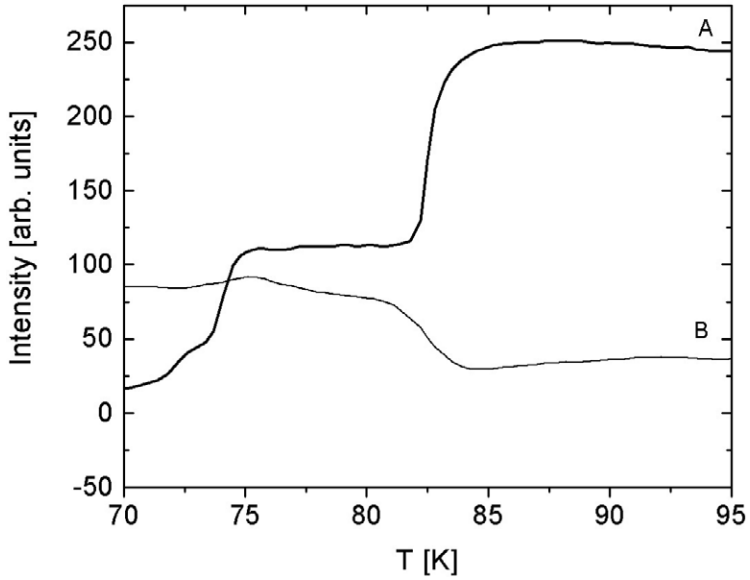

Figure 4. LEED adsorption isobars for substrate and overlayer diffraction intensities at $P = 6.5 \times 10^{-6}$ mbar. These curves have not been corrected for the Debye–Waller attenuation.

for at least two layers. These isobars were recorded with decreasing T. With decreasing T, the first vertical step corresponds to the adsorption of the first layer, and the second smaller step corresponds to the adsorption of the second layer. A third step is apparent in a few isobars at the higher P, T range. The percentage intensity attenuation of the substrate diffraction from the first layer adsorption is somewhat larger than that observed for Xe/Ag(111) [8], about 60% compared to 50%, which may be due to different background subtraction methods, or the fact that Pb is a weaker scatterer than Ag due to its larger Debye–Waller factor. For similar pressures, the formation of the monolayer, and to a lesser extent the second layer, occurs at somewhat lower temperatures than for Xe/Ag(111), indicating weaker adsorption.

When the monolayer starts to adsorb, a set of new diffraction spots appears in the LEED pattern. These correspond to a hexagonal incommensurate structure of Xe/Pb(111) that is aligned with the substrate lattice, but has a larger unit cell. These spots are azimuthally elongated (see figure 2), similar to those observed for Xe on Ag(111), which is also an aligned incommensurate monolayer [9]. Both the alignment and the azimuthal elongation are thought to arise from the Xe overlayer nucleating and growing from the step edges that are not perfectly straight. To characterize their evolution during the adsorption, the intensities of those overlayer spots were compared to those of the substrate spots. Figure 4 shows these intensities for one adsorption isobar at $P = 6.5 \times 10^{-6}$ mbar. The curve labelled 'A' corresponds to the substrate spot intensity, already shown in figure 3. The curve labelled 'B' is the intensity of the Xe spots which appear during the adsorption of the first layer, indicating that the Xe orders upon adsorption at these temperatures. Their intensities decrease somewhat when the second layer of Xe adsorbs. We note that there is a greater degree of rounding at the onset of the first-layer step, compared to the second-layer step, indicating that some heterogeneity in the Xe–surface potential is reduced for the second layer [10].

The heats of adsorption can be determined from the isobars shown in figure 2. Figure 5 shows Arrhenius plots of the P, T points for 0.5 layer and 1.5 layer coverages. From the slopes

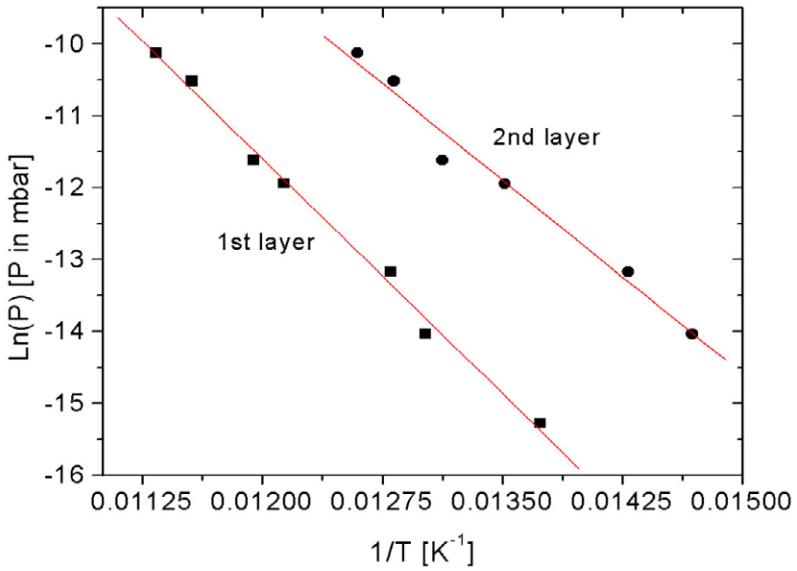

Figure 5. Isosteres for 0.5 and 1.5 layers, taken from isobars for decreasing T. The heats of adsorption determined from these isosteres are given in table 1.

Table 1. Isosteric heats of adsorption for Xe on Pb(111).

Xe coverage	Heat of adsorption (meV)
0.5 layers	191 ± 10
1.5 layers	158 ± 20

of these curves, the heats of adsorption were derived using [8]

$$q_{\mathrm{st}} = -k_{\mathrm{B}} \left. \frac{\mathrm{d}(\ln P)}{\mathrm{d}(1/T)} \right|_{\theta},$$

where the pressure at the sample at low T is corrected from the value measured in the gauge at room temperature by using the thermomolecular correction factor

$$P_{LT} = P_{RT} \sqrt{\frac{T_{LT}}{T_{RT}}}.$$

The heats of adsorption are given in table 1. The heat of adsorption for the second layer (158 meV) is comparable to that of bulk Xe (161 meV [8]) and suggests that bulk growth may occur as early as the second or third layer in this temperature range, and may account for the lack of definite steps for the lower P isobars shown in figure 3. Earlier photoemission measurements of Xe on Pb(111) suggested a Stranski–Krastanov growth mode at $T \approx 20$ K, with two full layers followed by 3D growth [11].

From the LEED data taken during the equilibrium isobars, it is also possible to measure the coefficient of thermal expansion for the monolayer [8]. The thermal expansion coefficient determined from such equilibrium experiments is given by

$$\alpha = \left. \frac{1}{L} \frac{\partial L}{\partial T} \right|_{P} = \left. \frac{\partial \ln(L)}{\partial T} \right|_{P}$$

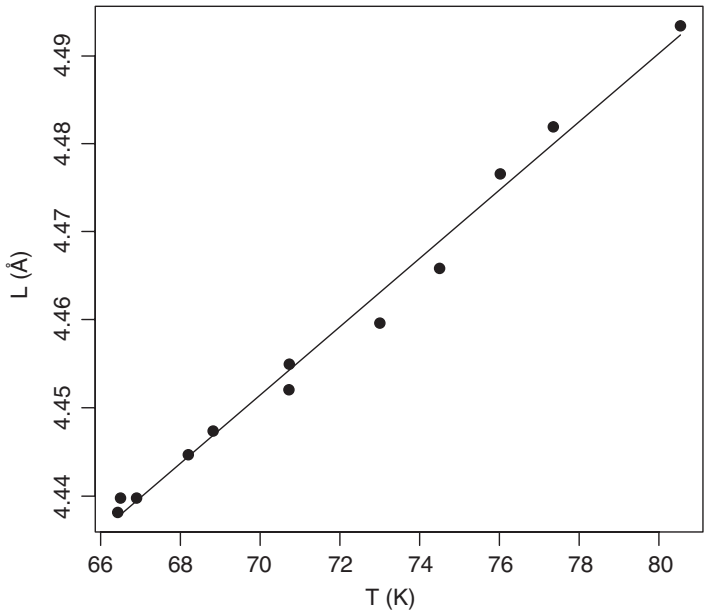

Figure 6. Temperature dependence of the natural log of the Xe–Xe spacing L as a function of T for the constrained monolayer, measured relative to the Pb–Pb spacing, taken from four different isobars. The linear fit to $\ln(L)$ is also shown, and the expansion coefficient, corrected for the Pb expansion, is given in table 2.

Table 2. Linear thermal expansion coefficients and isothermal compressibilities (2D) for adsorbed Xe.

Adsorption system	α ($\times 10^{-4}$ K^{-1})	κ_T (m^2 J^{-1})
Xe/Pb(111) (at 75 K)	9 ± 1	0.76 ± 0.13
Xe/Ag(111) (at 80 K) [8, 12]	20 ± 2	0.71 ± 0.12
Bulk Xe (at 75 K) [13]	2.2	—

where L is the nearest-neighbour Xe–Xe spacing in the monolayer. Using this equation, the isobaric thermal expansion coefficient can be determined from the slope of the $\ln(L)$ versus T plot, as shown in figure 6. The value of the coefficient of thermal expansion for Xe/Pb(111) is given in table 2, along with a corresponding value for the similar system of Xe/Ag(111) [8, 12]. A value for the thermal expansion coefficient was also obtained for the unconstrained Xe layer (i.e. $P = 0$) in the temperature range $T = 15$–50 K. This was $3.5 \pm 0.5 \times 10^{-4}$ K^{-1}, and compares to values obtained for Xe/Ag(111) of 1.5–4.5×10^{-4} K^{-1} in a similar range of T [8].

The temperature dependence of the diffraction intensity from the unconstrained layer allows vibrational parameters of the Xe layer to be determined. Experiments were performed for both heating and cooling between 10 and 50 K using an electron beam energy of 99 eV. The decay of the intensity of the diffraction spots with T is given by

$$I \propto \mathrm{e}^{-2M}$$

where

$$2M = \frac{S_\perp^2 \langle u_\perp^2 \rangle}{T} + \frac{S_\parallel^2 \langle u_\parallel^2 \rangle}{T}.$$

Because the momentum transfer in a LEED experiment is dominated by the perpendicular

Table 3. Vibrational parameters for Xe obtained from the temperature dependence of the diffraction intensities. The incident electron beam was at normal incidence, $E = 99$ eV.

Parameter	Xe/Pb(111)
$\langle u_\perp^2 \rangle / T$ (m^2 K^{-1})	$2.7 \pm 0.1 \times 10^{-24}$
$\langle u_\perp^2 \rangle^{1/2}$ at 50 K (Å)	0.12 ± 0.01
Debye T (K)	37 ± 2
Bulk Xe Debye T (K)	55
E_{vib} (meV)	3.2 ± 0.3

component, the vibration amplitude obtained from these experiments is assumed to be the perpendicular component. The vibration energy obtained thus corresponds to the perpendicular vibration and is obtained using $E = \hbar\omega_\perp$, where

$$\tfrac{1}{2} m\omega_\perp^2 \langle u_\perp^2 \rangle = \tfrac{1}{2} k_B T.$$

The mean square vibration amplitude at 50 K and the perpendicular vibration energy thus calculated for Xe are given in table 3. The mean square vibrational amplitude can be related to the Debye temperature of the surface, Θ_D, by

$$\langle u^2 \rangle = \frac{3\hbar^2 T}{m k_B \Theta_D^2}.$$

The Debye temperature for adsorbed Xe, calculated assuming isotropic vibrations, is given in table 3.

3.2. Overlayer–substrate spacing

The fact that the Xe monolayer is incommensurate precludes a 'traditional' dynamical LEED analysis of its structure. No satellite intensities were observed in the LEED patterns from Xe/Pb(111) that would be expected if there were a significant modulation of the density of the overlayer due to the substrate; therefore it is assumed that the Xe layer is relatively uniform at the temperatures studied here, and that the Xe occupies all possible sites on the substrate. In order to determine the Xe–Pb spacing, we have used a constant-momentum-transfer analysis (CMTA), which is a well-established method for analysing LEED data [14, 15] and has been used previously for other incommensurate layers [12, 16, 17]. The CMTA method involves enhancing the kinematic aspects of LEED intensity spectra by averaging spectra measured under different scattering conditions. These pseudo-kinematic spectra can then be transformed directly in order to determine structural parameters. The procedures followed for the data analysis are described in [17].

The data for this study consist of intensity spectra for the specular beam taken at four different angles from 0° to 14° off normal, and at a sample T of 78 K. Spectra were acquired for clean Pb(111) and for a monolayer of Xe. The spectra were then plotted as a function of perpendicular momentum transfer and averaged, resulting in the curves shown in figure 7(a). The intensity curves were then divided to produce a curve for the intensity ratio, $I_{\text{Xe/Pb}}/I_{\text{Pb}}$, as shown in figure 7(b), and as described in [17], the dominant oscillation in the spectrum is expected to be due to the overlayer–substrate spacing. A Fourier transform (FT) of this curve is shown in figure 7(c). The FT is somewhat distorted at the lower perpendicular distance (R) values because of a low-frequency component that is introduced by the mismatch of the period of oscillations with the length of the dataset. This was overcome by 'padding' the data with zeros to have a total length of 100 $Å^{-1}$, thus shifting the interference effects to much lower R values. The resulting FT with the padding is shown in figure 7(d). The dominant peak in this

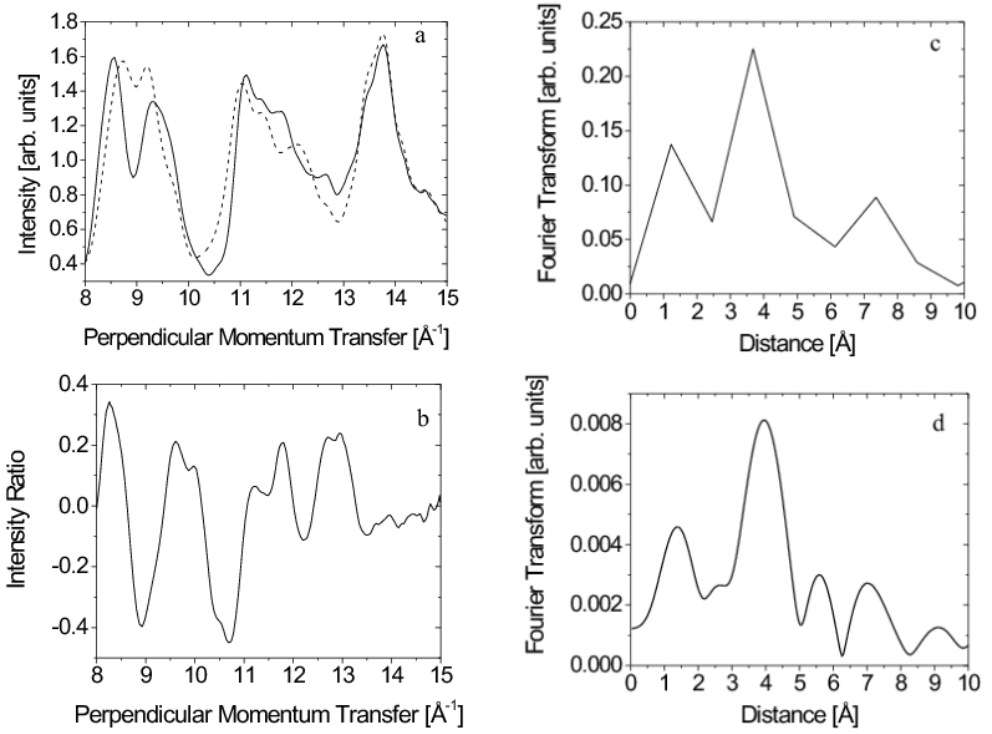

Figure 7. (a) Averaged LEED intensity spectra for clean Pb(111) (dashed) and for one monolayer of Xe (solid) on Pb(111). (b) Ratio of the Xe/Pb(111) intensity and the Pb(111) intensity curves shown in (a). A DC component has been subtracted. (c) Fourier transform (FT) of the spectrum in (b). (d) FT from the padded spectrum.

spectrum, at about 4 Å, corresponds to the Xe–Pb interlayer spacing. The next largest one at about 1.3 Å corresponds to the difference between the Xe–Pb spacing and the Pb–Pb spacing. The location of the peaks in the FT can in principle be shifted by the phase shifts of the atomic scattering factors [17], but including phase shifts in this analysis made no significant change to the result because the phase shifts had very similar functional dependences on energy. Fitting the peak near 4 Å results in a final value of 3.95 ± 0.10 Å for the Xe–Pb interlayer spacing.

4. Discussion and conclusions

The isobars shown in figure 3 suggest the possibility that the Xe may begin to form bulk crystallites after two layers are adsorbed, at least for the lower T range of our measurements. This may not be surprising, given that the heat of adsorption is lower than for Xe on any surface measured so far, with the possible exception of Al(110) [18] and for alkali metals [19]. A low heat of adsorption also is not particularly surprising since the Pb atoms are much larger than most other metals (the lattice constant of Pb is 4.95 Å, compared to 4.09 Å for Ag and 3.61 Å for Cu), meaning that the repulsive Xe–Pb interaction prevents the Xe from approaching the deeper part of the attractive holding potential. One consequence of the low heat of adsorption is that Xe may not wet the Pb(111) surface, and from the measured isobars, it appears that the resolution of the steps corresponding to the formation of the second and higher layers becomes

Table 4. Experimental values for perpendicular adsorption distances of Xe on various substrates. R_{eff} is the effective radius of Xe on the substrate, equal to the perpendicular distance minus the substrate radius determined from its bulk structure (or the van der Waals radius in the case of graphite). q_{st} is the heat of adsorption, typically for a coverage between 0.5 and 1 monolayer.

Substrate	Structure/site	d_z (Å)	R_{eff} (Å)	q_{st} (meV)
Pb(111)	Incommensurate/mixed	3.95	2.2	191
Cu(110)	c(12 × 2)/mixed	3.3 [22]	2.02	218 [23]
Ag(111)	Incommensurate/mixed	3.55 [12]	2.1	225 [8]
Cu(111)	$(\sqrt{3} \times \sqrt{3})$R30°	3.6 [24]	2.32	227 [25]
Ru(0001)	$(\sqrt{3} \times \sqrt{3})$R30°	3.54 [26]	2.19	230 [27]
Graphite	$(\sqrt{3} \times \sqrt{3})$R30°	3.59 [28]	1.86	239 [29]
Pt(111)	$(\sqrt{3} \times \sqrt{3})$R30°	3.4 [30]	2.02	298 [31]
Pd(111)	$(\sqrt{3} \times \sqrt{3})$R30°	3.07 [32]	1.68	320 [33]

indistinct at the lower temperatures measured. At all temperatures measured here, however, the Xe adsorbs as an ordered incommensurate hexagonal monolayer.

The coefficient of linear thermal expansion of the constrained Xe layer from this study is about half that measured earlier in the LEED studies of Xe on Ag(111), which forms a similar incommensurate structure [12]. The smaller value found for Xe/Pb might be attributed to a slightly less repulsive interaction between Xe atoms on Pb, and we note that, for the same T, the lattice spacing of Xe on Pb(111) is slightly smaller (up to 0.03 Å) than on Ag(111). This is consistent with the lower temperatures for the onset of adsorption measured for Xe on the Pb surface compared to Ag, which implies weaker binding. A weaker binding energy would produce a smaller dipole moment for the Xe atoms, leading to less dipole–dipole repulsion, which is soft compared to the repulsive atom–atom interaction from charge overlap, and therefore a smaller expansion coefficient. The expansion coefficients for both monolayers, however, are larger than the measured bulk value [13]. The value obtained for zero P (unconstrained layer) is similar to that obtained for Xe/Ag(111) and is smaller than the constrained value, as expected, since the spreading pressure is zero.

As a substrate, Pb(111) poses some challenges for diffraction studies because of its low Debye temperature. It is already known that the large vibration amplitudes of adsorbed Xe can hinder precise measurements of the geometrical parameters [5], and adding the large vibration amplitudes of Pb leads to unusually weak diffraction intensities from the Xe monolayer. The average perpendicular vibration amplitude of Xe measured from the Debye–Waller factor at 50 K is 0.12 ± 0.01 Å, which is similar to values found for Xe on other substrates [5]. The corresponding perpendicular vibration energy is 3.2 ± 0.3 meV, similar to values obtained in He-atom scattering experiments from Xe on other metal surfaces [5, 20].

The measured perpendicular distance between the Xe and the Pb(111) is quite large, but when the large size of the Pb atoms is taken into account, it is consistent with other measurements of Xe–metal distance. Table 4 gives values for the measured perpendicular Xe–surface spacings for several systems, along with their heats of adsorption. Also given are values for the effective radius of Xe that is obtained by subtracting the radius of the substrate metal atoms from the perpendicular distance. In the case of the top site structures, these values represent the Xe radius. Our justification for applying the same method to the other structures is that calculations indicate that the perpendicular spacing of the Xe above the surface has little dependence on the site, even in the case of graphite [21]. Figure 8 shows the effective radius of Xe plotted against the heat of adsorption. It can be seen that there is a general trend for the effective Xe radius to decrease with increasing adsorption energy. Such a trend was also observed in the DFT calculations for Xe on metal surfaces [6].

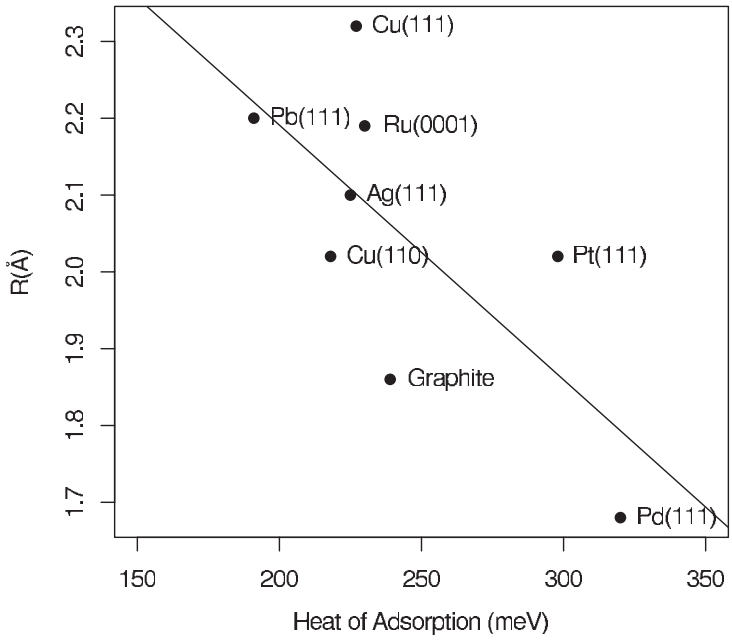

Figure 8. Effective Xe radius (see table 4) as a function of the monolayer heat of adsorption. The line is a fit to the data.

To summarize, the parameters obtained from this LEED study of adsorption of Xe on Pb(111) fit within the general framework established by earlier studies on other similar substrates such as Ag(111). Like Xe on Ag(111), Xe on Pb(111) forms an incommensurate structure that is aligned with the substrate. Although the preferred site could not be determined from these studies, the lack of satellite intensities in the LEED patterns suggests that the overlayer is quite uniform, further suggesting that the corrugation is small. The binding of Xe to Pb(111) is weaker than for other substrates, probably related to the large size of the Pb atoms. It would be useful to have other measurements and also DFT calculations for Xe and other gases on Pb(111), particularly since there is considerable interest in the frictional properties of gases on Pb at low temperatures [34–36].

Acknowledgments

We thank L W Bruch for stimulating our interest in this system, Franco Jona for providing us with Pb crystals, and Gil Alexandrowicz for useful advice on FTs. This material is based upon work supported by the National Science Foundation under Grant Nos 0208520 and 0505160.

References

[1] Lazic P, Crljen Z, Brako R and Gumhalter B 2005 *Phys. Rev.* B **72** 245407
[2] Dion M, Rydberg H, Schroder E, Langreth D C and Lundqvist B I 2004 *Phys. Rev. Lett.* **92** 246401
[3] Tkatchenko A and von Lilienfeld O A 2006 *Phys. Rev.* B **73** 153406
[4] Bruch L W, Cole M W and Zaremba E 1997 *Physical Adsorption: Forces and Phenomena* (Oxford: Oxford University Press)

[5] Diehl R D, Seyller T, Caragiu M, Leatherman G S, Ferralis N, Pussi K, Kaukasoina P and Lindroos M 2004 *J. Phys.: Condens. Matter* **16** S2839
[6] Da Silva J L F, Stampfl C and Scheffler M 2005 *Phys. Rev.* B **72** 075424
[7] Leatherman G S and Diehl R D 1996 *Phys. Rev.* B **53** 4939
[8] Unguris J, Bruch L W, Moog E R and Webb M B 1979 *Surf. Sci.* **87** 415
[9] Leatherman G S, Diehl R D, Karimi M and Vidali G 1997 *Phys. Rev.* B **56** 6970
[10] Dash J G and Puff R D 1981 *Phys. Rev.* B **24** 295
[11] Jacobi K 1988 *Phys. Rev.* B **38** 5869
[12] Cohen P I, Unguris J and Webb M B 1976 *Surf. Sci.* **58** 429
[13] Tilford C R and Swenson C A 1972 *Phys. Rev.* B **5** 719
[14] Pendry J B 1972 *J. Phys. C: Solid State Phys.* **5** 2567
[15] Lagally M, Ngoc T C and Webb M B 1971 *Phys. Rev. Lett.* **26** 1557
[16] Shaw C G, Chinn M D, Fain S C Jr and Toney M F 1980 *Surf. Sci.* **97** 128
[17] Fisher D, Li Z Y and Diehl R D 1991 *Surf. Sci.* **259** 85
[18] Zeppenfeld P 2001 *Landolt Boernstein: Physics of Covered Surfaces* vol III/42A, ed H P Bonzel (Berlin: Springer) p 67
[19] Chizmeshya A, Cole M W and Zaremba E 1998 *J. Low Temp. Phys.* **110** 677
[20] Graham A P 2003 *Surf. Sci. Rep.* **49** 115
[21] Chen X R, Zhou X L, Zhu J and Gou Q Q 2003 *Phys. Lett.* A **315** 403
[22] Caragiu M, Seyller T and Diehl R D 2003 *Surf. Sci.* **539** 165
[23] Pouthier V, Ramseyer C, Girardet C, Diercks V, Halmer R, David R and Zeppenfeld P 1998 *Phys. Rev.* B **57** 13149
[24] Seyller T, Caragiu M, Diehl R D, Kaukasoina P and Lindroos M 1998 *Chem. Phys. Lett.* **291** 567
[25] Jablonski A, Eder S, Markert K and Wandelt K 1986 *J. Vac. Sci. Technol.* **4** 1510 (This paper did not establish the heat of adsorption for Xe/Cu(111), but identified it to be between the heats of adsorption for Xe/Ag(111) and Xe/Ru(0001), which are reported to be 225 meV and 230 meV, respectively, in this table. We have thus taken the heat of adsorption to be 227 meV.)
[26] Narloch B and Menzel D 1998 *Surf. Sci.* **412/413** 562
[27] Schichting H and Menzel D 1992 *Surf. Sci.* **272** 27
[28] Pussi K, Smerdon J, Ferralis N, Lindroos M, McGrath R and Diehl R D 2004 *Surf. Sci.* **548** 157
[29] Suzanne J, Coulomb J P and Bienfait M 1975 *Surf. Sci.* **47** 204
[30] Seyller T, Caragiu M, Diehl R D, Kaukasoina P and Lindroos M 1999 *Phys. Rev.* B **60** 11084
[31] Lehner B, Hohage M and Zeppenfeld P 2002 *Phys. Rev.* B **65** 165407
[32] Caragiu M, Seyller T and Diehl R D 2002 *Phys. Rev.* B **66** 195411
[33] Zhu J F, Ellmer H, Malissa H, Brandstetter T, Semrad D and Zeppenfeld P 2003 *Phys. Rev.* B **68** 045406
[34] Bruch L W 2000 *Phys. Rev.* B **61** 16201
[35] Bruschi L, Fois G, Pontarollo A, Mistura G, Torre B, Buatier de Mongeot F, Boragno C, Buzio R and Valbusa U 2006 *Phys. Rev. Lett.* **96** 216101
[36] Dayo A, Alnasrallah W and Krim J 1998 *Phys. Rev. Lett.* **80** 1680